INJURY BIOMECHANICS RESEARCH
Proceedings of the Fortieth International Workshop

Evaluation of Head Injury: Extent and Distribution of Extra-axial Lesions from Motor Vehicle Crashes

Jillian E Urban, Sarah K Lynch, Elizabeth M Lillie, and Joel D Stitzel

ABSTRACT

Approximately 1.7 million people sustain a traumatic brain injury (TBI) each year, with motor vehicle crash (MVC) representing the leading cause for TBI-related hospitalization. Subarachnoid hemorrhage (SAH), subdural hematoma (SDH), cerebral contusion, and diffuse axonal injury (DAI), are some of the most common and serious consequences of MVC-related TBI and are associated with high mortality and morbidity rates. Little is known, however, about the relationship between the contact location on the head and resulting intracranial trauma. Contact location between the head and internal components of the vehicle were used in the analysis of hemorrhage extent and distribution in order to better understand occupant injury, with the hypothesis that the common contacts for occupants in MVCs would correlate with specific hemorrhage patterns.

Head computed tomography (CT) scans demonstrating cerebral SAH (42), SDH (33), contusion (25), and/or DAI (12) were selected from the Crash Injury Research Engineering Network (CIREN) database. Semi-automated methods were used to quantify intracranial volume, extent and distribution, and approximate contact location identified from a soft tissue scalp contusion. Label maps representing the injured volume and the scalp contusion were converted to three-dimensional (3D) point clouds. The 3D data from each occupant was aligned to a global spherical coordinate system using bony landmarks identified on the skull. Incremental calculation of injury volume was performed at 0.2 radian by 0.2 radian increments along the azimuth and elevation axes of the spherical coordinate system. The volume was calculated from a 3D Delaunay triangulation to create a polygonal surface of the convex hull of the points. Injury distribution and extent was quantified in terms of theta (about SAE Z-axis) and phi (from the SAE XY-plane) in relation to the contact location.

This study is the first volumetric analysis of real-world head injuries using clinical CT and known crash characteristics with contact information. These data highlight the utility of combining clinical neuroimaging with mechanical crash data for investigating mechanisms of TBI. Results from this study will allow for a better understanding of the biomechanics of traumatic brain injury. Such data may be used in the future for the validation of finite element models of the head to better mitigate and prevent head injury.

INTRODUCTION

Head injuries from motor vehicle crashes (MVCs) are the leading cause of hospitalization and death for the population (Faul, M., Xu, L. et al. 2010). Nearly 1.7 million people sustain a traumatic brain injury (TBI) annually, with approximately 16% resulting in hospitalization and 3% resulting in death (Faul, M., Xu, L. et al. 2010). The most common manifestations of head injury include subarachnoid hemorrhage (SAH), subdural hematoma (SDH), cerebral contusion, and diffuse axonal injury (DAI). Although each injury is classified as a 'head injury', the clinical presentation, anatomic location within the head, and the mechanism of each injury differs. The location of head injuries within the skull can be intraparenchymal, such as cerebral contusion or DAI, or extra-axial, such as SDH, SAH, and epidural hematoma (EDH). Along with the varied location of the injury within the head, the extent and distribution may vary, as well. Many factors that may play a role in the manifestation of the injury include acceleration type (linear vs. rotational acceleration), impact location, impacted surface, or impact duration (Weaver, A. A., Danelson, K. A. et al. 2012).

TBI is an acceleration-based injury, often resulting from direct contact or loading to the head (Nirula, R., Mock, C. et al. 2003; Yoganandan, N., Baisden, J. L. et al. 2010). Focal injuries such as cerebral contusion have been correlated with contact loading (Gennarelli, T. A. and Meaney, D. F. 1996). Although the mechanism of more diffuse type injuries, such as DAI, is unclear, more recent studies utilizing the Crash Injury Research Engineering Network (CIREN) have demonstrated that the loading mechanism is most commonly associated with head impact resulting from direct contact (Yoganandan, N., Gennarelli, T. A. et al. 2009; Yoganandan, N., Baisden, J. L. et al. 2010). The CIREN database contains detailed vehicle, crash, and medical data on injured MVC occupants (NHTSA 2010) and has proven to be a valuable resource for documenting and understanding the mechanisms of injuries. It contains pre-crash information, along with detailed scene and vehicle investigation, medical images and injury causation scenario (ICS) and patient outcome. Patient injuries are coded using AIS and ICD-9.

Quantification of the extent and distribution of head injuries with respect to contact locations is a useful tool for the understanding of head injury mechanisms. Previous studies by have utilized neuropathic examination of post-mortem brains to assess injury location within the brain (Ryan, G. A., McLean, A. J. et al. 1994; Gorrie, C., Duflou, J. et al. 1999; Gorrie, C., Duflou, J. et al. 2001). In a previous study by Ryan et al, the brain was sectioned into 109 sectors and the extent of hemorrhage within each sector was measured to evaluate the percentage of brain sectors with injury. From the study, the vulnerability of the frontotemporal regions during occipital impacts was identified. Although the methods developed in the study are valuable for assessing injury extent and distribution, they are only applicable for post-mortem evaluation of serious head injury that resulted in death. Therefore, it is imperative to develop methods for evaluating the extent and distribution from medical imaging data collected for a wide variety of head injury severities.

This study utilizes image segmentation of head injuries from real world crashes in order to develop methods to quantify extent and distribution of head injuries from medical imaging. The objective of this study is to quantify the extent and distribution of head injury and correlate the contact location with the resulting injury location for four different head injuries: SAH, SDH, cerebral contusion, and DAI. The information presented in this study may ultimately be used to relate data from real world crashes to finite element modeling (FEM) in order to validate the strain distribution observed from simulated head impacts. These data are important to understand the mechanisms of head injuries, specifically on a per-injury basis.

METHODS

Axial non-contrast head computed tomography (CT) data within the first 24 hours post-crash and radiology reports were collected for cases with CT data within the CIREN database demonstrating SAH, SDH, and cerebral contusion based on 1998 (AAAM 2001) and 2005 (AAAM 2008) AIS coding. CT data for cases containing DAI were selected based on 2005 (AAAM 2008) AIS coding. Soft tissue algorithm CT data were selected for this study to optimize visualization of intracranial blood products (Bruce, D. A. 2000). Detailed data regarding the occupant, injury, vehicle, and crash were also collected. In the CIREN database, involved physical components (IPCs) are the objects thought to be contacted by the occupant considered to play a role in producing an injury. The IPCs are designated as “certain,” “probable,” and “possible” based on

the confidence level of the reviewers and specific evidence-based coding guidelines from vehicle crash, occupant kinematics, and injury evidence. Vehicle data included: vehicle year, make, model, manual belt use, collision deformation classification (CDC) code, and airbag deployment for the associated occupant seating location. Crash type, delta-v, and barrier estimate speed (BES) were also collected for the highest severity impact. Rollover cases were excluded from the analysis. Data were collected using the CIREN SQL interface and SQL developer (Oracle, Redwood Shores, CA). All cases selected underwent a full case review with medical, engineering, and crash reconstruction specialists to determine injury causation. Quality control checks have been undertaken, and the cases are designated as "complete" in the database.

Image Segmentation

Head CT scans were segmented using manual and semi-automated techniques within Mimics version 14 (Materialise, Leuven, Belgium). Segmentations were conducted based on density thresholds of bone (skull) and soft tissue (intracranial and skin). All brain injuries were identified from descriptions within the radiology reports and verified by a board-certified neuroradiologist. The SDH, SAH, cerebral contusion, DAI and additional intracranial injuries were segmented using a semi-automated method to identify the hemorrhage within the appropriate layer of the brain (extra-axial, intraparenchymal, or within cerebrospinal fluid (CSF) filled spaces). Injury segmentations were reviewed by a board certified neuroradiologist to ensure proper volume identification of the injury.

Figure 1. Image segmentation and three-dimensional (3D) reconstruction example. (A) Axial CT image of occupant with SAH. (B) Image segmentation of SAH.

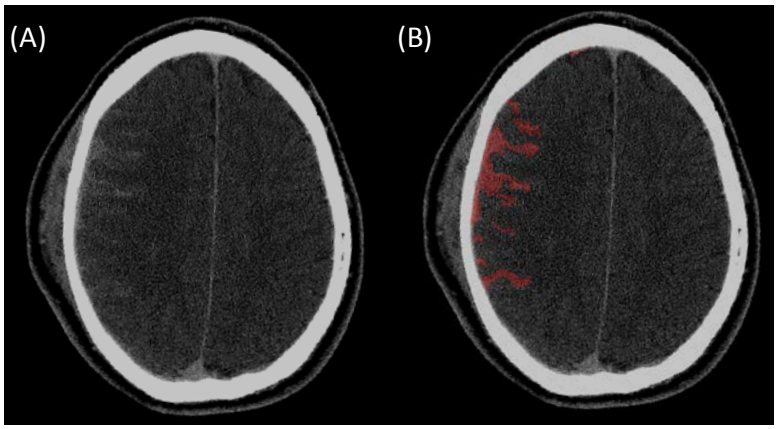

The point of contact between the head and vehicle was identified by the presence of a superficial soft tissue/scalp contusion on the CT images and on the three-dimensional (3D) CT reconstructions of the skin. The 3D reconstruction of the skin was isolated to the location of swelling and converted to a point cloud. The centroid of the soft tissue swelling point cloud was calculated and interpreted to be the approximate location of contact. If swelling did not occur, the point of contact on the head was approximated by the IPC, ICS, anticipated occupant kinematics, and de-identified occupant photos.

Injury Extent and Distribution

A local head coordinate system (Figure 2A) was established from bony landmarks that were identified from the 3D reconstruction of the occupant skull. The bony landmarks were at the left and right external auditory meatus (EAM) and nasion. The axis of the local coordinate system was determined from the perpendicular intersection of the nasion landmark projection on the line between the left and right EAM. This point was established as the origin of the local head coordinate system. The local x-axis was defined as the vector between the origin and nasion and the local y-axis was defined as the vector defined between the origin and the right EAM. The z-axis was determined from the cross product between the x- and y-axis so that the local coordinate system was in the SAE configuration. In the event that a head CT scan did not contain any of the bony landmarks, the scan of interest was co-registered with a scan of an occupant with bony landmarks using surface registration. The respective bony landmarks were then assumed to be coincident between the two occupants. Each occupant local head coordinate system was aligned to a global coordinate system using a transformation matrix defined by translations and rotations.

The transformation matrix between the local and global coordinate systems were applied to 3D data of the injury and soft tissue swelling and then converted to a spherical coordinate system. Incremental calculation of injury volume was performed at 0.2 radian by 0.2 radian increments along the azimuth and elevation axes of the spherical coordinate system. Each 0.2 radian by 0.2 radian increment is referred to as an injury sector. Label maps representing the injured volume and the scalp contusion were converted to 3D point clouds. The injury volume was calculated from a 3D Delaunay triangulation to create a polygonal surface of the convex hull of the points within each injury sector and projected onto the surface of a unit sphere established from the normalized distance between the left and right EAM (Figure 2B). A polygonal surface defined by the convex hull is the smallest enclosed space around the point cloud within the injury sector from which the volume is calculated. Injury distribution and extent was quantified in terms of theta (about SAE Z-axis) and phi (from the SAE XY-plane), respectively. Lastly, the spherical coordinate system was divided into eight regions, as shown in Figure 2C to determine the generalized contact location with respect to the injury location. Injuries were evaluated per injury type.

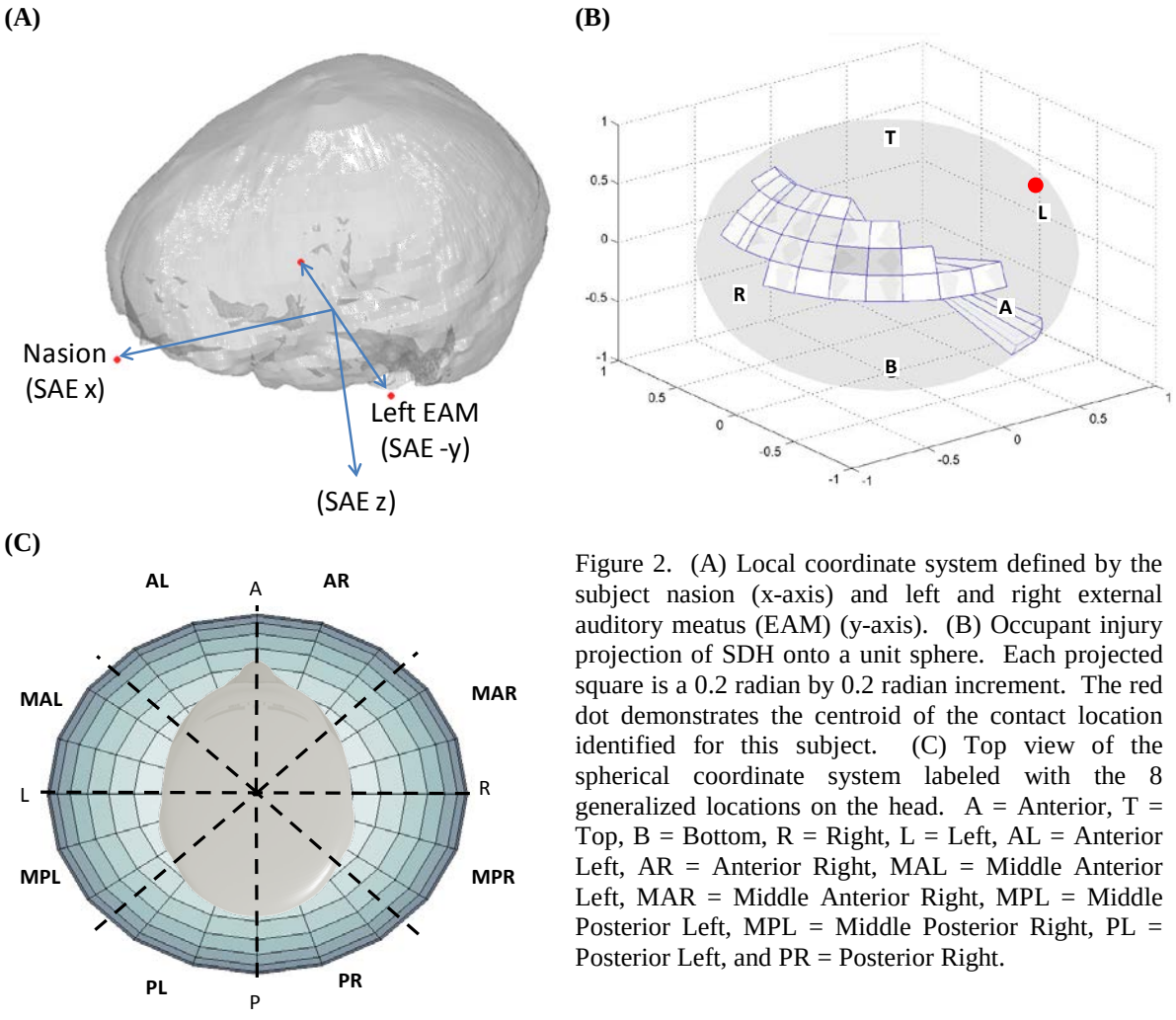

Figure 2. (A) Local coordinate system defined by the subject nasion (x-axis) and left and right external auditory meatus (EAM) (y-axis). (B) Occupant injury projection of SDH onto a unit sphere. Each projected square is a 0.2 radian by 0.2 radian increment. The red dot demonstrates the centroid of the contact location identified for this subject. (C) Top view of the spherical coordinate system labeled with the 8 generalized locations on the head. A = Anterior, T = Top, B = Bottom, R = Right, L = Left, AL = Anterior Left, AR = Anterior Right, MAL = Middle Anterior Left, MAR = Middle Anterior Right, MPL = Middle Posterior Left, MPL = Middle Posterior Right, PL = Posterior Left, and PR = Posterior Right.

Orthodromic distance was used to calculate the 3D spherical distance between the centroid of the contact location and the primary injury location. This value was used to assess the location of the injury with respect to the contact location. The orthodromic distance (d) is defined as the shortest path between two points on a sphere (Equation 1). The volume of injury within each injury sector was projected onto the surface of a unit sphere. The primary location of injury was identified as the median injury sector location for SDH. The primary location of injury was identified as the injury sector with the highest percentage of

blood compared to the rest of the injury for SAH and cerebral contusion. The orthodromic distance was calculated between the contact location centroid (θ_c, φ_c) and the primary location of injury (θ_i, φ_i). Occupant CT data was assessed visually and labeled as coup or contrecoup. A receiver operating characteristic (ROC) curve analysis was performed that related *coup/contrecoup* grouping as a function of orthodromic distance. The goal was to determine the orthodromic distance threshold that discriminates between coup and contrecoup injuries. The orthodromic distance value with the greatest area under the receiver operator characteristic (AUROC) was determined to be the optimal distance threshold to discriminate between coup and contrecoup injuries.

$$d = acos^{-1}[\cos(90-\varphi_c)\cos(90-\varphi_i)\cos(\theta_c-\theta_i) + sin(90-\varphi_c)\sin(90-\varphi_i)] \quad \text{(Equation 1)}$$

where a is the radius of the sphere (a = 1 for unit sphere)

RESULTS

Of occupants in the CIREN database with head injuries, there were 92 cases with adequate soft tissue CT data collected within 24 hours post-crash demonstrating the injury. Of the 92 cases, 21 cases had mixed head injuries of the type targeted for this study and 71 had isolated head injuries with a total of 42 cases with SAH, 33 cases with SDH, 25 cases with cerebral contusion, and 12 cases with DAI. Occupant and crash data is provided in Table 1. Each of the head injuries were segmented and the contact location was identified for each occupant. All injury segmentations were verified by a board certified neuroradiologist.

Table 1. Summary of the crash and occupant data collected for the 92 occupants with head injury. SAH = subarachnoid hemorrhage, SDH = subdural hematoma, DAI = diffuse axonal injury. Data presented as mean (standard deviation).

Injury	n	M/F	Age	Delta V (kph)	Frontal/Side	Driver/Pass	Belted/ Unbelted
SAH	42	20/22	42.3 (± 19.32)	40.1 (± 22.2)	16/26	41/1	30/14
SDH	33	16/17	40.0 (± 23.7)	36.9 (± 14.71)	13/20	30/3	27/6
Cerebral Contusion	23	14/9	39.4 (± 17.14)	36.1 (± 11.58)	6/17	21/2	17/6
DAI	12	6/6	25.9 (± 15.2)	48.5 (± 28.1)	5/7	10/2	9/3

The extra-axial injuries include SAH and SDH. The most common coded IPCs for occupants with SAH include the A-Pillar, B-Pillar, and Door Panel with soft tissue swelling in the frontotemporal (MAL) region. The injury locations were similarly found to be in same hemisphere as the contact location within the frontotemporal regions of the head. The injury sectors defined by the SAH were made of multiple disconnected injury sectors. The distribution and extent of injury was found to span the cerebral convexities with an average distribution of 81.4 (±48.7) degrees and extent of 60.2 (±39.7) degrees. Those occupants with SDH most commonly contacted the A-Pillar and B-Pillar with blood products from the SDH distributed along the cerebral convexities. These were identified by continuous adjacent sectors of injury with an average distribution and extent of 183.2 (±51.5) degrees and 80.0 (±42.4) degrees, respectively. The most common contact locations were within the frontotemporal (MAL) and temporal (MPL) regions of the head. The SDHs most commonly resulted in a contrecoup injury, however 44% of the occupants had blood products contained within the falx cerebri and tentorium cerebelli regions of the brain.

Intraparenchymal injuries studied include cerebral contusion and DAI. Occupants with cerebral contusion were most commonly coded as contacting the A-Pillar, B-Pillar, or window frame. Soft tissue swelling was most commonly found in the frontal (AL) region of the head. Cerebral contusions were focally located in the basal frontal and temporal regions of the brain with an average distribution of 84.4 (±70.9) degrees and extent of 32.7 (±25.5) degrees. The most common contact locations for those occupants with DAI were the steering wheel rim and steering wheel through airbag. Many of those occupants with DAI

required further investigation of the approximate contact location based on occupant kinematics or facial or scalp abrasions from occupant photos. Additionally, the DAI was dispersed with no relative pattern with respect to the contact location within subjects, however many occupants did have patterns of concentrated DAI within the corpus callosum. The injury was distributed throughout the brain with an average distribution of 107.9 (± 87.9) degrees and extent of 70 (±29.7) degrees.

The proximity to impact location was assessed by the orthodromic distance between the contact location and injury location. The average orthodromic distance from the contact location to the injury location is provided in Table 2 for SAH, SDH, and cerebral contusions. The orthodromic distance was not determined for DAI due to the dispersion of the injury through the brain and approximate contact location. The ROC curve analysis demonstrates an orthodromic distance threshold between injury location and contact location that may distinguish between coup and contrecoup injuries is 52˚ with an AUROC of 0.85732. This would be the equivalent of a quarter of a hemisphere of the head with coup injuries occurring generally in the same quadrant as the impact location. More specifically, any injury more than one quadrant away or often in the quadrant adjacent to the impact location would generally be classified as contrecoup.

Table 2. Spherical measurements for each injury type including distribution, extent, number of injury sectors, and orthodromic distance.

Metric	SAH	SDH	Contusion	DAI
Distribution (degrees)	81.4 (±48.7)	183.2 (±51.5)	84.4 (±70.9)	107.9 (± 87.9)
Extent (degrees)	60.2 (±39.7)	80.0 (±42.4)	32.7 (±25.5)	70 (±29.7)
# Injury Sectors	29.8 (± 31.4)	39.4 (± 29.7)	8.60 (± 9.56)	17.75 (± 18.36)
Orthodromic Distance (degrees)	59.6 (± 29.3)	43.0 (± 46.0)	58.4 (± 32.4)	N/A

CONCLUSIONS

This study quantifies the extent and distribution of SAH, SDH, cerebral contusion, and DAI volume. Additionally, the injury location relative to the contact location was assessed. Extra-axial injuries, such as SAH and SDH, were distributed along the cerebral convexities with SAH being more diffuse and SDH more focally confined to a single location in the head (i.e., right or left cerebral convexity, falx cerebri). Intraparenchymal injuries, such as contusion and DAI, differed with cerebral contusions often focally located within the frontotemporal region of the brain and DAI distributed throughout the brain. DAI was, however often concentrated in the region of the corpus callosum.

Diffuse and focal injuries were observed for both extra-axial and intraparenchymal injuries. Those occupants with SAH had multiple disconnected sectors, suggesting that the distribution of blood is not continuous and is more diffuse in nature. However, the blood products of this injury were centrally located within approximately one quarter (<90 degree distribution) of the cerebral convexities, as well as within the basal cisterns. Interestingly, the injury was within the same hemisphere as the contact location, however the average orthodromic distance measured between the contact location and the highest concentration of injury for SAH was found to be greater than the coup/contrecoup threshold, suggesting that this injury is commonly a more contrecoup-type injury. On the contrary, those occupants with SDH had multiple continuous adjacent injury sectors distributed along the cerebral convexities. From this, it is concluded that the blood products from SDH are focally located within a single hemisphere of the head or within the falx. Only the more severe impacts resulted in bilateral SDH.

Cerebral contusion was most commonly the result of a frontal impact to the head, with the injury focally located in the frontotemporal regions of the brain. Cerebral contusion had the least number of injury sectors and the small distribution and extent. These data agree with findings presented by previous literature with regard to cerebral contusion (Courville, C. B. 1950; Gurdjian, D. I. 1975; Bigler, E. D. 2007). A previous hypothesis by Bigler et al has been presented regarding the increased vulnerability of the frontal and temporal lobe in high speed impacts. His hypothesis is that there is an increased vulnerability due to the

concavities of the skull base (Bigler, E. D. 2007). The results of this study support this hypothesis. Lastly, DAI was sparsely distributed throughout the brain with a large distribution and extent with little continuity of injury sectors. Many of the occupants had contact locations that were approximated at the frontal region of the head, similar to cerebral contusions, with less similarities in injury location between subjects, however this limitation may be attributed to sample size (n = 13). It would be a valuable pursuit to further analyze the deformation within the frontotemporal regions of the brain in a FE model of the brain on a case by case basis. Ideally with a known injury location and approximated kinematics resulting from the impact, it is anticipated that the FE model would predict high strains in this region, as well. A database containing medical images from real world crashes with known occupant kinematics and evidence of contact location on both the vehicle and occupant is a valuable tool for analyzing and validating the strain response measured from a computational model.

This study introduced a method to quantify the distribution and extent of injury with respect to contact location using medical imaging of occupants from real world crashes. Four common head injuries were evaluated, particularly those with different manifestations (i.e. extra-axial vs intraparenchymal, focal vs. diffuse). These data highlight the utility of combining clinical neuroimaging with mechanical crash data for investigating mechanisms of TBI. Results from this study will allow for a better understanding of the biomechanics of traumatic brain injury. Such data may be used in the future for the validation of finite element models of the head to better mitigate and prevent head injury.

ACKNOWLEDGEMENTS

Work was performed for the Crash Injury Research and Engineering Network (CIREN) Project at Wake Forest University School of Medicine in cooperation with the United States Department of Transportation/National Highway Traffic Safety Administration (USDOT/NHTSA). Funding has been provided by National Highway Traffic Safety Administration under Cooperative Agreement Number DTNH22-09-H-00265 and DTNH22-10-H-00294. Views expressed are those of the authors and do not represent the views of NHTSA. Previous funding of the Wake Forest University CIREN center has been provided by Toyota Motor North America Inc under Cooperative Agreement Number DTNH22-05-H-61001. The authors would like to acknowledge Kathryn Loftis for help with scan acquisition and SQL data download, Colston Edgerton, Rachel Austin, Kavya Reddy, Andrew Chambers, Pavani Thotakura, and Nicole Angelo for assistance in image segmentation, and Landon Edward and Christopher Whitlow for assistance in review of the image segmentations. Additionally, thank you to the CIREN collaborating centers.

REFERENCES

AAAM (2001). "Abbreviated Injury Scale 1990 (Updated 1998)." Association for the Advancement of Automotive Medicine.

AAAM (2008). "Abbreviated Injury Scale 2005 (Updated 2008)." Association for the Advancement of Automotive Medicine.

BIGLER, E. D. (2007). "Anterior and middle cranial fossa in traumatic brain injury: relevant neuroanatomy and neuropathology in the study of neuropsychological outcome." Neuropsychology **21**(5): 515-531.

BRUCE, D. A. (2000). "Imaging after head trauma: why, when and which." Childs Nerv Syst **16**(10-11): 755-759.

COURVILLE, C. B. (1950). Pathology of the central nervous system. Mountain View, CA.

FAUL, M., XU, L., et al. (2010). Traumatic brain injury in the United States: emergency department visits, hospitalizations, and deaths. N. C. f. I. P. a. C. Centers for Disease Control and Prevention. Atlanta.

GENNARELLI, T. A. and MEANEY, D. F. (1996). Mechanisms of Primary Head Injury Neurosurgery. W. R and R. S. New York, McGraw Hill**:** 2611-2621.

GORRIE, C., DUFLOU, J., et al. (2001). "Extent and distribution of vascular brain injury in pediatric road fatalities." J Neurotrauma **18**(9): 849-860.

GORRIE, C., DUFLOU, J., et al. (1999). "Fatal head injury in children: a new approach to scoring axonal and vascular damage." Childs Nerv Syst **15**(6-7): 322-328.

GURDJIAN, D. I. (1975). Impact head injury: Mechanistic, clinical and preventive correlation. Springfield, IL.

NHTSA (2010). Crash Injury Research and Engineering Network Coding Manual. Department of Transportation, National Highway Traffic Safety Administration.

NIRULA, R., MOCK, C., et al. (2003). "Correlation of head injury to vehicle contact points using crash injury research and engineering network data." Accid Anal Prev **35**(2): 201-210.

RYAN, G. A., MCLEAN, A. J., et al. (1994). "Brain injury patterns in fatally injured pedestrians." J Trauma **36**(4): 469-476.

WEAVER, A. A., DANELSON, K. A., et al. (2012). "Modeling Brain Injury Response for Rotational Velocities of Varying Directions and Magnitudes." Ann Biomed Eng.

YOGANANDAN, N., BAISDEN, J. L., et al. (2010). "Severe-to-fatal head injuries in motor vehicle impacts." Accid Anal Prev **42**(4): 1370-1378.

YOGANANDAN, N., GENNARELLI, T. A., et al. (2009). "Association of contact loading in diffuse axonal injuries from motor vehicle crashes." J Trauma **66**(2): 309-315.